CORRELATION OF FAR-INFRARED EMISSION AND RADIO CONTINUUM EMISSION ALONG THE MAJOR AXIS OF EDGE-ON SPIRAL GALAXIES

B. HEIKKILA AND W.R. WEBBER
Astronomy Department, New Mexico State University, Las Cruces, NM 88003

ABSTRACT Using new High Resolution far-infrared (FIR) images we have determined FIR flux densities, the FIR luminosity, and intensity profiles along the major axis for eight nearby edge-on spiral galaxies. We present spatial comparisons between the FIR profiles in three of the four IRAS Bands (25, 60, 100 μm). We also present direct spatial comparisons between the 60 μm intensity profiles and intensity profiles from 20 cm radio continuum maps with identical resolution ($\sim 60''$) obtained from J.J. Condon. Using these profiles we have evaluated the 60 μm-to-20 cm ratio Q_{60} along the major axis for each galaxy and have compared the results to global Q_{60} values. This analysis reveals that a considerable amount of complicated structure exists within the disks of spiral galaxies. Closer examination of this disk structure will make it possible to place further constraints on the well known global far-infrared and radio continuum emission correlation.

INTRODUCTION

The discovery, in the early eighties, of the tight correlation between integrated thermal far-infrared emission and non-thermal radio continuum emission from spiral galaxies (Dickey and Salpeter 1984) has prompted numerous studies to see if the correlation holds spatially within the disks of individual spiral galaxies (e.g. Beck and Golla 1988; Bicay and Helou 1990). These studies, however, have been hampered by the lack of resolution in the far-infrared images. The development of the new High Resolution (HiRes) processing capabilities of the Infrared Processing and Analysis Center (IPAC) has resulted in far-infrared images with a five-fold increase in resolution compared with previous maps produced by the Full Resolution Survey Coadder (FRESCO). This increased resolution allows the infrared detections made by IRAS to be analyzed in greater detail than previously possible. In addition, the resolution of the 60 μm maps ($\sim 60''$ at 20 iterations) is almost exactly the same as the resolution of the National Radio Astronomy Observatory Very Large Array (VLA) in D-array at 20 cm. We have used this unique resolution relationship to directly compare the 60 μm far-infrared distribution and the 20 cm (predominantly non-thermal) radio continuum emission in a sample of spiral galaxies. Studies concerning the global far-infrared radio correlation (e.g. Devereux and Eales 1989; Chi and Wolfendale

S. Terebey and J. Mazzarella (eds.), *Science with High-Spatial Resolution Far Infrared Data*, 95–100, 1994, Jet Propulsion Laboratory, Pasadena, CA.

1990) have shown that the emission mechanisms for the far-infrared and radio continuum are most probably linked through massive star formation. It is the goal of this present study to try to understand this relationship better.

GALAXY SAMPLE

For this initial part of our analysis we have selected eight nearby (D< 20 Mpc) edge-on ($i > 75°$) spiral galaxies of morphological type Sb or later. The HiRes processing also required that the sources be sufficiently bright with flux densities greater than ~ 2 MJy/Sr and sufficiently sampled by IRAS with at least 2 all-sky Hours-Confirmation scans. The list of selected galaxies, inclination, far-infrared luminosity, L_{fir}, evaluated using

$$L_{fir} = 3.94 \times 10^5[2.58S_{60\mu m}(Jy) + S_{100\mu m}(Jy)]D^2(Mpc)L_{\odot} \quad (1)$$

(*Cataloged Galaxies and Quasars Observed in the IRAS Survey* 1985) and the integrated flux densities from the 25, 60 and 100 μm HiRes images are shown in Table 1. Also shown are published 20 cm flux densities (Condon 1987) and the global 60 μm-to-20 cm ratio Q_{60} for each galaxy.

TABLE 1 Luminosity and Integrated Fluxes

Galaxy	i [a]	L_{FIR} (1×10^9)	Flux Density (Jy) 25 μm	60 μm	100 μm	20 cm	Global Q_{60}
NGC 4565	90°	2.42	0.94	9.62	40.42	0.131	73.44
NGC 5907	90°	7.78	1.15	13.79	53.42	0.089	154.94
NGC 4157	90°	10.15	1.31	15.56	49.02	0.242	64.22
NGC 4517	90°	1.42	0.60	6.71	20.25	0.036	186.39
NGC 4631	85°	7.06	7.33	79.50	171.17	1.200	66.25
NGC 0891	84°	12.27	5.75	63.57	173.80	0.701	90.68
NGC 3556	81°	10.14	3.27	30.07	51.93	0.306	98.27
NGC 2683	79°	0.60	0.54	7.22	28.25	0.066	109.39

[a]Inclination (Tully 1988)

DATA ANALYSIS

For each galaxy in our sample, a cut, averaged over 3 pixels ($\sim$45″), was made along the major axis defined by the optical position angle. The same cuts were made on the 25, 60, and 100 μm maps as well as the 20 cm radio continuum images (Condon 1992).

The 25 μm and 100 μm major axis intensity profiles were numerically scaled to the 60 μm profile to try to identify structure such as peaks or "hot spots" within the dust distribution in the disk of each spiral galaxy. The peaks show up predominantly in the 25 μm profile due to the increased resolution and higher dust temperatures associated with this band. These peaks may be tracers of

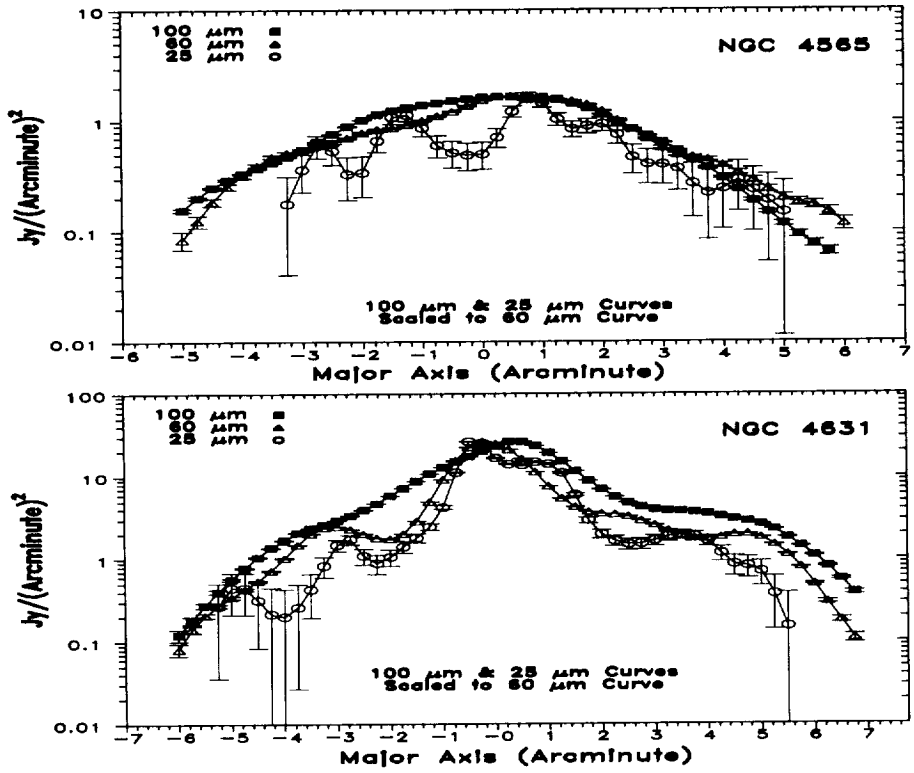

FIGURE 1 Example 25, 60, and 100 μm Major Axis Profiles

giant HII regions within spiral arms. The major axis profiles extend out to the 5σ noise level determined from the maps, and the error bars represent the 1σ noise in the individual data points. Profiles for two galaxies are shown in Figure 1. In this figure the resolution along the major axis is $\sim 45''$ for the 25 μm profile, $\sim 60''$ for the 60 μm profile, and $\sim 75''$ for the 100 μm profile.

For each galaxy the 60 μm cuts are then compared to the 20 cm major axis profiles determined in exactly the same way. These comparisons are shown in Figure 2 and Figure 3 for all eight galaxies. We then calculated Q_{60} ($S_{60\mu m}/S_{20cm}$) values along the major axis. These profiles are also shown in Figure 2 and Figure 3 along with the global Q_{60} values represented by a dashed line. The 1σ errors in these figures are approximately the size of the data points. These Q_{60} profiles show considerable structure. At this early stage of data analysis using both the Q_{60} profiles and the individual 60 μm and 20 cm profiles (and before a similar study of face-on galaxies) we believe there is evidence for two classes of galaxies. NGC 2683 and NGC 4157 show a strongly decreasing Q_{60} profile as well as decreasing 60 μm and 20 cm profiles along the major axis. For these galaxies it appears that the IR and radio emission are both concentrated in the center. If the sources of electrons that are producing the radio emission are concentrated in the center then the decreasing Q_{60} profile may be explained by the outward diffusion of these electrons.

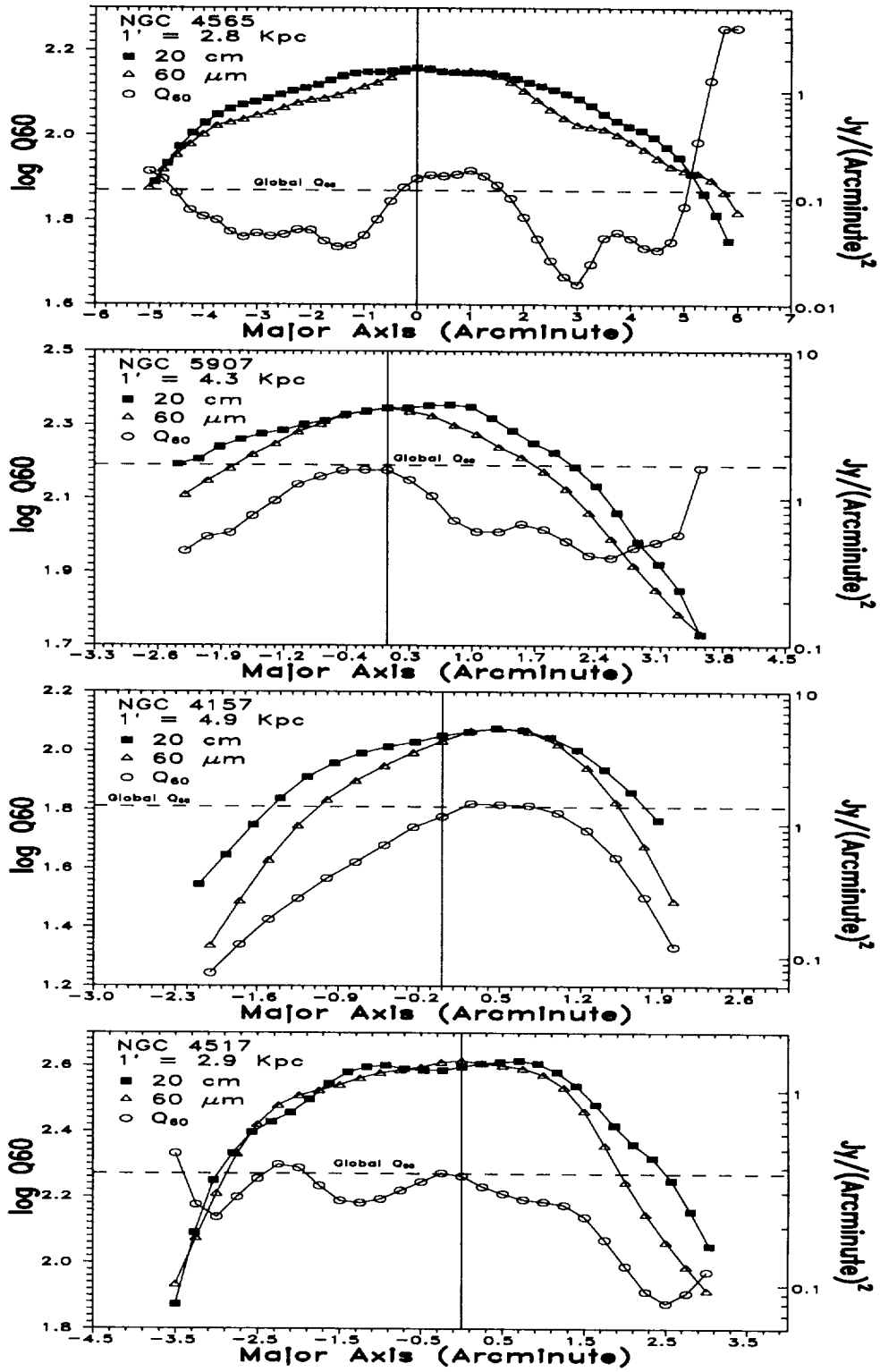

FIGURE 2 60 μm 20 cm Comparison Profiles and Q_{60} Values

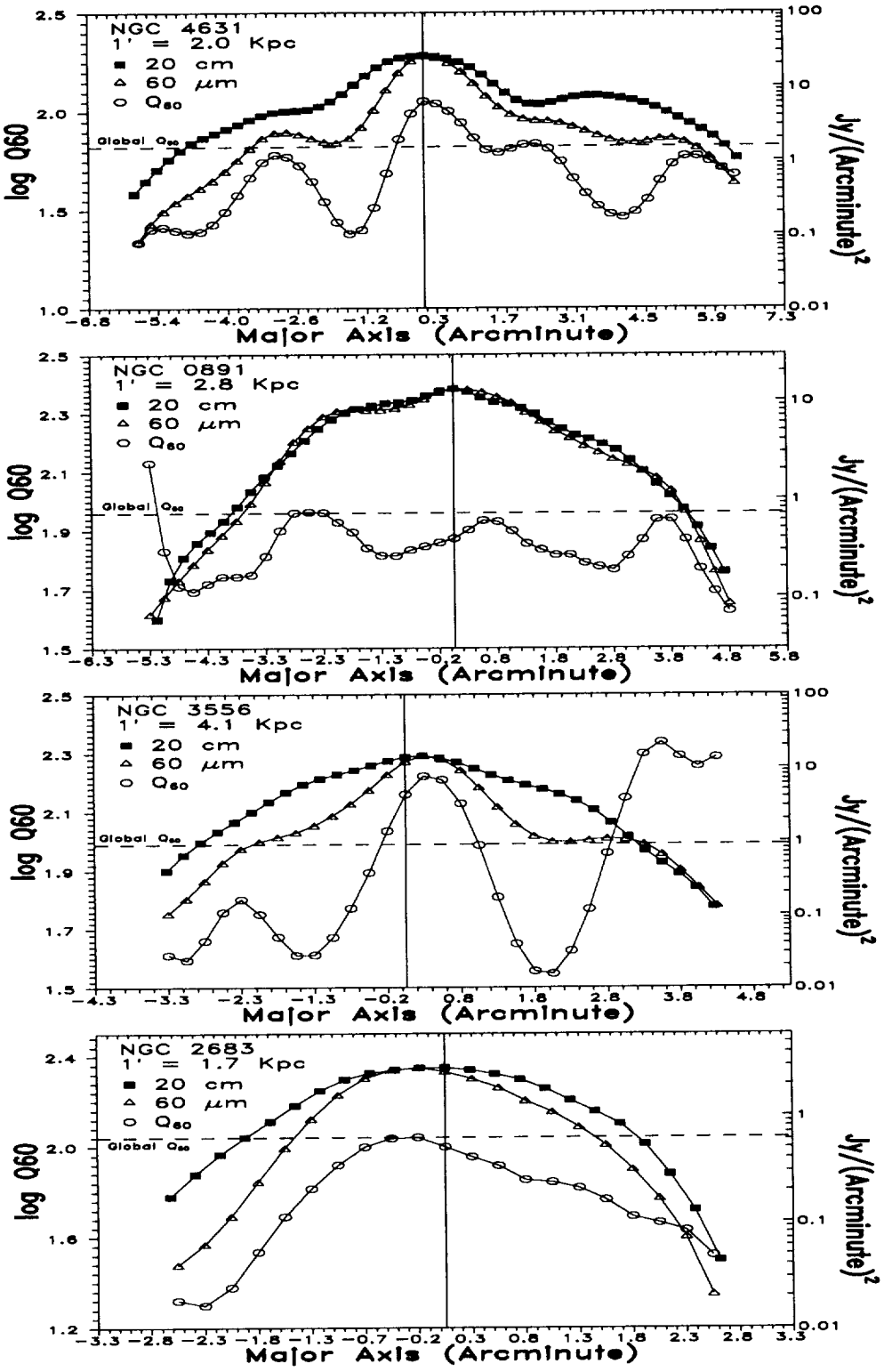

FIGURE 3 60 μm 20 cm Comparison Profiles and Q_{60} Values

The other six galaxies show more complicated Q_{60} profiles but basically they can be interpreted in terms of an almost constant Q_{60} ratio out to the distance at which both the 60 μm and 20 cm profiles decrease rapidly - e.g., the edge. Some galaxies have more structure on top of this constant profile than others and some such as NGC 3556 and NGC 4631 appear to have a central 60 μm peak as well which gives the appearance of a central bulge in the Q_{60} profile. All of these galaxies may be interpreted in terms of the sources of the electrons that are producing the radio emission being more uniformly distributed in radius out to the edge, beyond which both the 60 μm and 20 cm radiation decrease rapidly.

CONCLUSIONS

The global FIR Radio correlation for an individual galaxy will be affected by the relative contributions from the the disk and central bulge components to the total FIR and Radio emission. Our analysis shows a more complicated structure within these components than previously indicated. In particular, the 25 μm major axis profiles show numerous peaks within both the central bulge and disks of spiral galaxies. These "hot spots" are probably associated with recent star formation.

The Q_{60} profiles show considerable structure. A preliminary analysis of these profiles suggests two classes of galaxies — one in which the radio and IR emission is concentrated in the center and the outward diffusion of electrons is responsible for the decreasing Q_{60} profile — the other in which most of the radio and IR emission is distributed more uniformly out to the edge. The Q_{60} ratio in these galaxies can be thought of as roughly constant upon which considerable structure exists including a separate central IR bulge in some cases.

ACKNOWLEDGMENTS

We are grateful to J.J. Condon for providing us with 20 cm VLA maps.

REFERENCES

Beck, R., and Golla, G. 1988, *ApJ*, **191**, L9

Bicay, M. D., and Helou, G. 1990, *ApJ*, **362**, 59

Cataloged Galaxies and Quasars Observed in the IRAS Survey, 1985, prepared by C. J. Lonsdale, G. Helou, J. C. Good, and W. Rice

Chi, X., and Wolfendale, A. W. 1990, *MNRAS*, **245**, 101

Condon, J. J. 1987, *ApJS*, **65**, 485

Condon, J. J. 1992, *Private Communication*

Devereux, N. A., and Eales, S. A. 1989, *ApJ*, **340**, 708

Dickey, J. M., and Salpeter, E. E. 1984, *ApJ*, **284**, 461

Tully, R. B. 1988, *The Nearby Galaxies Catalog*, (Cambridge University Press)